

ROBUST NONUNIFORMITY CORRECTION IN INFRARED IMAGES BASED ON GLOBAL MOTION

Marlene Shehadeh, Oleg Kuybeda

Electrical Engineering Dept. Technion - Israel Institute of Technology
Technion City, Haifa 32000, Israel

ABSTRACT

The presence of spatial and temporal fixed pattern noise (FPN) due to nonuniformity in sensor parameters is a well known problem in IR focal plane detector arrays. In order to obtain a noise-free image, the nonuniformity parameters should be estimated and compensated for. This work presents a scene-based nonuniformity correction (NUC) algorithm that estimates and compensates the nonuniformity parameters by equalizing output of different detectors that were exposed to the same information. The correspondence between pixels is found via an improved robust global motion estimation technique that locates and excludes local motion and occlusion regions from the estimation of motion parameters. The performance of the proposed algorithm is evaluated both in image sequences with simulated fixed-pattern noise and real infrared image sequences. Significant reduction in FPN is demonstrated in both cases.

1. INTRODUCTION

Infrared imaging systems are widely used for a variety of applications in astronomy, defense, surveillance, etc. Many infrared detectors are based on Infrared Focal Plane Array (IRFPA) technology [1]. A notorious problem of this technology is that every detector in the array can have a different response to the same stimulus causing fixed pattern noise (FPN) in the resulting images [2]. In recent years a variety of non-uniformity correction (NUC) techniques have been proposed [3 - 15]. IRFPA sensors are commonly characterized by the following linear model:

$$y_{ij} = x_{ij} \cdot g_{ij} + o_{ij}, \quad (1)$$

where x_{ij} , y_{ij} , g_{ij} and o_{ij} are the incident radiance, output, gain and offset of a detector (i, j), respectively.

The simplest and the most accurate NUC procedures use uniform blackbody infrared sources as a reference to estimate detector parameters and compensate the non-uniformity. Thus, the authors of [3] propose a two-point calibration technique that uses two different temperature reference targets to calculate gain and offset parameters of each detector.

Unfortunately, methods based on temperature references require interrupting vision while the detector array is calibrated, which may be undesirable in many applications. Moreover, since the non-uniformity tends to drift over time as a function of ambient temperature, the NUC has to be performed on a regular basis, which makes the problem of the vision interruption even worse. Therefore, considerable research has been focused on developing adaptive scene-based NUC methods that need no temperature reference targets [4-15].

The NUC methods proposed in the literature can be classified according to assumptions that they make on the FPN characteristics and the FPN-free signal as follows: One group of methods is based on statistical assumptions on the FPN-corrected IRFPA output. For example, the authors of [4, 5] assume that all detector outputs have equal and constant means and variances; the authors of [6, 7] assume zero mean output of each detector; another assumption used in [8] is that the output of each detector accepts a constant range of values, equal for all detectors; the authors of [9] propose a Kalman filter based approach that exploits the constant range assumption and use a temporal stochastic model to describe gain and offset behavior in time; in [10,11] the variance of pixel values in local neighborhoods is assumed to be low. These methods work well with scenes characterized by constant and uniform dynamics, i.e., they satisfy the constant and uniform statistics assumptions. Unfortunately, many natural scenes don't obey these conditions. A striking example is an image that contains sky and ground which, obviously, have different means, whereas the horizon line is composed of non-uniform neighborhoods.

Another group of scene-based methods relies on motion estimation. Thus, algebraic scene-based NUC techniques, proposed in [12-14], assume equal outputs of detectors that are exposed to the same information. The pixel correspondences are found via a global motion estimation technique. The authors of [15] use a similar principle of equalizing detector outputs that are exposed to the same information based on optical flow. These methods are successful in a wider variety of scenes, since they don't make strict assumptions on the scene dynamics. However, their performance depends on how accurate the estimation of pixel correspondences is. Unfortunately, it is hard to obtain a precise correspondence of all pixels in the image since global motion, as well as optical flow based techniques, are not able to correctly identify the pixel correspondences in

occluded image areas, or in areas consisting of local motions [17]. Moreover, such areas may bias the registration results for other pixels. Registration techniques may be also misled by the FPN in smooth regions where the FPN contribution dominates the signal contribution. Once pixel correspondences are estimated, the FPN compensation parameters are estimated via minimizing an error function based on differences between the corresponding pixels.

In this paper, we adopt an iterative parameter estimation technique proposed in [11], which is denoted by the authors as adaptive neural network algorithm (ANN). The error function used in the ANN algorithm is equal to the difference between a pixel value and a mean of the pixel neighborhood. It is minimized using the least mean squares (LMS) algorithm [11, 21]. In contrast to the error function used by ANN, we employ an error function equal to the difference between the corresponding pixels in subsequent frames. The pixel correspondences are determined by a global motion estimation technique proposed in [16, 17]. In order to make the motion estimation process more robust, the contribution of the misleading areas such as occlusions and local motions which don't obey the global motion model, as well as smooth regions in which the FPN variance is stronger than the signal variance, are located and excluded from the registration process. After the registration is complete, the NUC parameters are estimated. During the parameter estimation process, problematic areas, such as occlusions and local motions, are also detected and excluded. The proposed algorithm is denoted as Robust NUC based on Global Motion (RNUC-GM). As we demonstrate on image sequences with simulated FPN and real FPN, RNUC-GM algorithm allows a better noise reduction in terms of SNR, as compared to the ANN algorithm.

2. ALGORITHM OUTLINE

First, we show an outline of the RNUC-GM algorithm. It is composed of a number of steps as illustrated in Fig.1. A preliminary global motion estimation is performed in subsequent frames (Fig.1 (a)). However, the preliminary motion estimation may contain errors due to possible occlusions and local motions that usually don't obey the global motion model. Moreover, in the presence of FPN, smooth areas in which the FPN variance is stronger than the signal variance may bias the motion estimation towards a zero motion, since the best match in these regions is obtained for zero motion. Therefore, in order to achieve a more accurate registration, a registration mask is created (Fig.1 (b)). It is then used to exclude the problematic regions from the motion estimation. Once the improved registration is achieved, it provides more reliable pixel correspondences in regions that obey the global motion model (Fig.1 (c)). Now, the NUC parameters can be estimated based on these pixel correspondences. It is important to note that we do include smooth regions in the NUC parameter estimation process, since smooth regions obey the global motion model.

All regions that participate in the estimation process are identified by a parameter estimation mask (Fig.1 (d)). Then, the NUC parameters estimation is iteratively performed by the LMS algorithm.

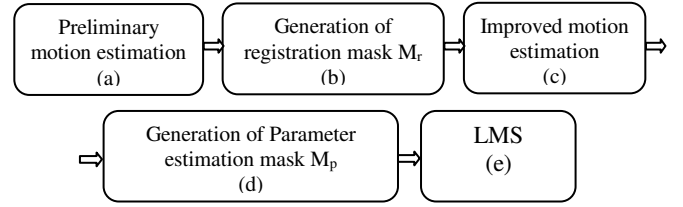


Figure1: RNUC-GM algorithm outline

2.1. Robust global motion estimation

In this section we describe the robust global motion estimation algorithm in detail. The preliminary motion estimation, as well as the improved motion estimation, is performed using the registration algorithm proposed in [16, 17]. According to it, the transformation between two consequent images $\mathbf{I}_k(i, j)$ and $\mathbf{I}_{k+1}(i, j)$ is modeled as follows:

$$\mathbf{I}_k(i, j) = \mathbf{I}_{k+1}(i \cos \theta - j \sin \theta + a, i \cos \theta + j \sin \theta + b), \quad (2)$$

where a, b and θ are horizontal shift, vertical shift and rotation angle, respectively, and k is the frame number. The parameters a, b and θ are estimated by minimizing the following cost function:

$$J(a, b, \theta) = \sum_{i, j \in \Omega} (\mathbf{I}_k(i, j) - \mathbf{I}_{k+1}(i \cos \theta - j \sin \theta + a, i \cos \theta + j \sin \theta + b))^2, \quad (3)$$

where Ω is the set of all pixel indices in the frame. As noted above, the minimization of J may lead to registration errors because of local motions, occlusions and FPN in smooth areas. To neutralize the effect of these areas, we propose a modified cost function:

$$\tilde{J}(a, b, \theta) = \sum_{i, j \in \Psi} (\mathbf{I}_k(i, j) - \mathbf{I}_{k+1}(i \cos \theta - j \sin \theta + a, i \cos \theta + j \sin \theta + b))^2. \quad (4)$$

Here the set of summation pixel indices Ω in (3) is replaced by a set Ψ , in which local motion regions and smooth regions are excluded. These regions are identified by a registration mask \mathbf{M}_r , which is obtained as follows:

$$\mathbf{M}_r = \mathbf{M}_s \cdot \mathbf{M}_l, \quad (5)$$

Here \mathbf{M}_s identifies smooth areas of the image, and \mathbf{M}_l identifies occlusions and local motion areas. An example of \mathbf{M}_s and \mathbf{M}_l obtained in a video sequence used in our simulations is shown in Fig. 2. Pixels with values equal to 0 belong to regions that \mathbf{M}_s and \mathbf{M}_l intend to exclude, whereas the rest of the image pixels receive the value of 1.

The generation of \mathbf{M}_s and \mathbf{M}_l is based on the global motion estimation results and is performed as follows: First, a preliminary motion is estimated between two subsequent frames \mathbf{I}_{k+1} and \mathbf{I}_k by minimizing the cost function J of (3). Then, we calculate a difference image \mathbf{D}_k as follows:

$$\mathbf{D}_k = \mathbf{I}_k - \hat{\mathbf{I}}_k, \quad (6)$$

where $\hat{\mathbf{I}}_k$ is a warped version of \mathbf{I}_{k+1} in the coordinate system

of \mathbf{I}_k . On one hand, since the local motions and occlusion regions don't obey the global model, they are expected to have high values in \mathbf{D}_k . On the other hand, the smooth regions have low values in \mathbf{D}_k . Therefore, local motions and occlusions are excluded by applying a high threshold equal to $1.5\hat{\sigma}_k$:

$$\mathbf{M}_l = \begin{cases} 1 & |\mathbf{D}_k| < 1.5\hat{\sigma}_k \\ 0 & |\mathbf{D}_k| \geq 1.5\hat{\sigma}_k \end{cases}, \quad (7)$$

whereas smooth regions are excluded by applying a low threshold equal to $0.5\hat{\sigma}_k$:

$$\mathbf{M}_s = \begin{cases} 1 & |\mathbf{D}_k| > 0.5\hat{\sigma}_k \\ 0 & |\mathbf{D}_k| \leq 0.5\hat{\sigma}_k \end{cases}. \quad (8)$$

Here $\hat{\sigma}_k$ denotes a robust estimation of the noise obtained as follows:

$$\hat{\sigma}_k = 1.3 \cdot \text{MAD}(\mathbf{D}_k), \quad (9)$$

where MAD denotes the median absolute deviation, which is proposed in [19] for a robust standard deviation estimation;

$$\text{MAD}(\mathbf{X}) = \text{median}(|\mathbf{X} - \text{median}(\mathbf{X})|). \quad (10)$$

The resulting global motion estimation is expected to be robust to errors that may be contributed by the presence of local motion, occlusion and smooth areas in the video sequence.

2.2. NUC parameters estimation

In this section we describe the proposed NUC parameter estimation process. As already noted above, a simple and accurate characterization of the sensor response is based on the following linear model:

$$y_{ij} = x_{ij} \cdot g_{ij} + o_{ij}, \quad (10)$$

where $x_{ij}, y_{ij}, g_{ij}, o_{ij}$ are the incident radiance, sensor response, gain and offset of a detector at a position (i, j) in the array, respectively. This model may be equivalently rewritten as:

$$x_{ij} = w_{ij} y_{ij} + b_{ij}, \quad (11)$$

where the parameters w_{ij} and b_{ij} are related to the gain and offset g_{ij} and o_{ij} as:

$$w_{ij} = \frac{1}{g_{ij}}, \quad b_{ij} = -\frac{o_{ij}}{g_{ij}}. \quad (12)$$

The parameter estimation is performed by minimizing the following function:

$$C = \sum_{i,j} (\hat{x}(i, j) - x(i, j))^2, \quad (13)$$

where $\hat{x}(i, j), x(i, j)$ are corresponding pixels from two subsequent frames, receiving identical incident radiance. According to the LMS algorithm proposed in [11] for the parameter estimation, w and b are updated as follows:

$$\begin{aligned} w_{ij}(k+1) &= w_{ij}(k) + \eta \cdot (x'_{ij}(k) - x_{ij}(k)) \cdot y_{ij}(k) \\ b_{ij}(k+1) &= b_{ij}(k) + \eta \cdot (x'_{ij}(k) - x_{ij}(k)) \end{aligned}, \quad (14)$$

where η is some fixed learning rate parameter, which controls the convergence rate of the algorithm. Smaller values of η give a more accurate but yet slower convergence. As mentioned above, the global motion estimation may produce incorrect

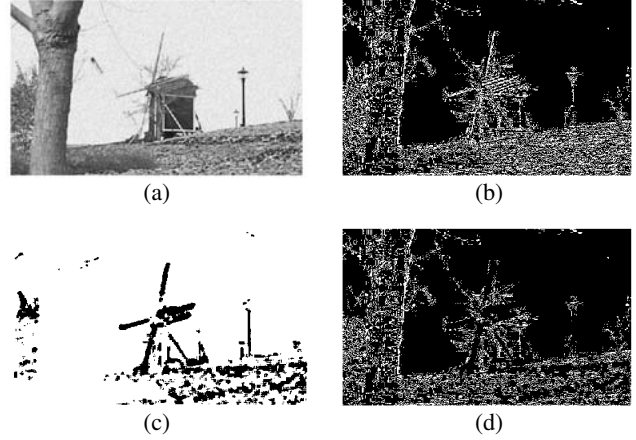


Figure 2: (a) original image with FPN (b) smooth areas mask \mathbf{M}_s (c) local motions and occlusions mask \mathbf{M}_l (d) combined mask \mathbf{M}_r , the black areas in each mask denote the excluded pixels.

pixel correspondences in regions of local motion or occlusions. Wrong pixel correspondences may introduce errors into the estimation of w and b , which makes the parameter estimation in these pixels undesirable. In order to avoid parameter updating in these areas, we use a mask \mathbf{M}_p obtained as follows:

$$\mathbf{M}_p = \begin{cases} 1 & |\tilde{\mathbf{D}}_k| < 2\tilde{\sigma}_k \\ 0 & |\tilde{\mathbf{D}}_k| \geq 2\tilde{\sigma}_k \end{cases}, \quad (15)$$

where $\tilde{\mathbf{D}}_k$ is a new difference frame generated after the improved motion estimation:

$$\tilde{\mathbf{D}}_k = \mathbf{I}_k - \tilde{\mathbf{I}}_k, \quad (16)$$

where $\tilde{\mathbf{I}}_k$ is obtained by warping the frame \mathbf{I}_{k+1} to the coordinate system of \mathbf{I}_k . Local motions and occlusions produce high values in the difference frame, therefore a threshold of $2\tilde{\sigma}_k$ is chosen. An example of the estimation mask is shown in Fig. 3.



Figure 3: Parameter estimation mask \mathbf{M}_p . Zero valued areas (black areas) correspond to local motions and occlusions in which the parameter update is suppressed.

3. RESULTS

In order to evaluate the proposed algorithm we use a video sequence "coastguard" obtained from the website in [20] that consists of 300 frames, which was duplicated back and forth to create a video sequence of 3300 frames. The simulated FPN was obtained by generating uniformly distributed gains $g \sim U[0.95 \ 1.05]$ and offsets $o \sim U[-0.05 \ 0.05]$, where $U[a, b]$ denotes the uniform distribution on the interval $[a, b]$. Before

correcting NUC parameters, the video sequence was linearly adjusted by bringing the maximum value to 1. The results of the proposed RNUC-GM algorithm were compared to the results of the ANN algorithm [11]. The last frame from the original image sequence is shown in Fig. 4 (a). A version containing synthetic FPN of the same frame is shown in Fig. 4 (b). The corrected frame by RNUC-GM is shown in Fig. 4 (d), whereas the corrected frame by ANN algorithm is shown in Fig. 4 (e). It can be noticed that the ANN algorithm produces blurring and ghosting effects in the area surrounding the boat and behind the boat, which are successfully eliminated by RNUC-GM algorithm, whereas in smooth regions, such as water and coastline, similar correction is attained by both algorithms.

In Fig. 5, we compare results of both algorithms in terms of SNR improvement as a function of frame number. Both algorithms were supplied with the same simulated FPN, corresponding to the initial SNR of 24 dB. The RNUC-GM algorithm managed to overcome the changes in the image (mainly resulting from local motion), achieving most of the correction after 1500 frames, and a total SNR improvement of 8dB. As can be seen in fig. 5, the ANN achieved a poorer SNR improvement of 1.5dB, since it was unable to adjust the NUC parameters very well in the regions that contain edges.

In order to examine the effectiveness of using masks in the RNUC-GM algorithm, a version of the proposed approach without using masks (denoted here by GR) was examined. In Fig. 5, one can see that the GR algorithm converges faster, achieving better results during the first 1000 frames, but at the same time, it is much more sensitive to local motions entering the scene. The GR achieved 5.5 dB SNR improvement, which

is approximately 2 dB less than what was obtained by RNUC-GM.

The RNUC-GM algorithm was also applied to a real data sequence counting 1000 frames obtained from an 8-12 micron IR camera. Frame 1000 from the original image sequence is displayed in Fig. 4 (c), versus the same frame after correction by the RNUC-GM algorithm, as shown in Fig. 4 (f); the noise lines appearing throughout Fig. 4 (c) and the strong noise in the middle of the frame vanish in Fig. 4 (f), giving a smooth clean image, especially in the lower part of the image.

4. CONCLUSION

In this paper we propose a new scene-based FPN correction approach, which uses a robust global motion estimation technique to match pixels exposed to the same information in an IR video sequence to estimate the nonuniformity correction parameters. The proposed technique uses masks during registration and estimation process. The registration mask is used to exclude the contribution of the misleading areas such as occlusions, local motions and smooth regions from the motion estimation, making it more robust. The estimation mask prevents estimating NUC parameters in local motion or occlusion areas, where the global motion is not able to produce correct pixel correspondences. This makes the parameter estimation more accurate.

The RNUC-GM was applied on a video sequence with simulated FPN as well as on a video sequence with real FPN. The real data and simulated the results demonstrate a significant reduction in FPN compared with both ANN and the RNUC-GM without using masks (GR).

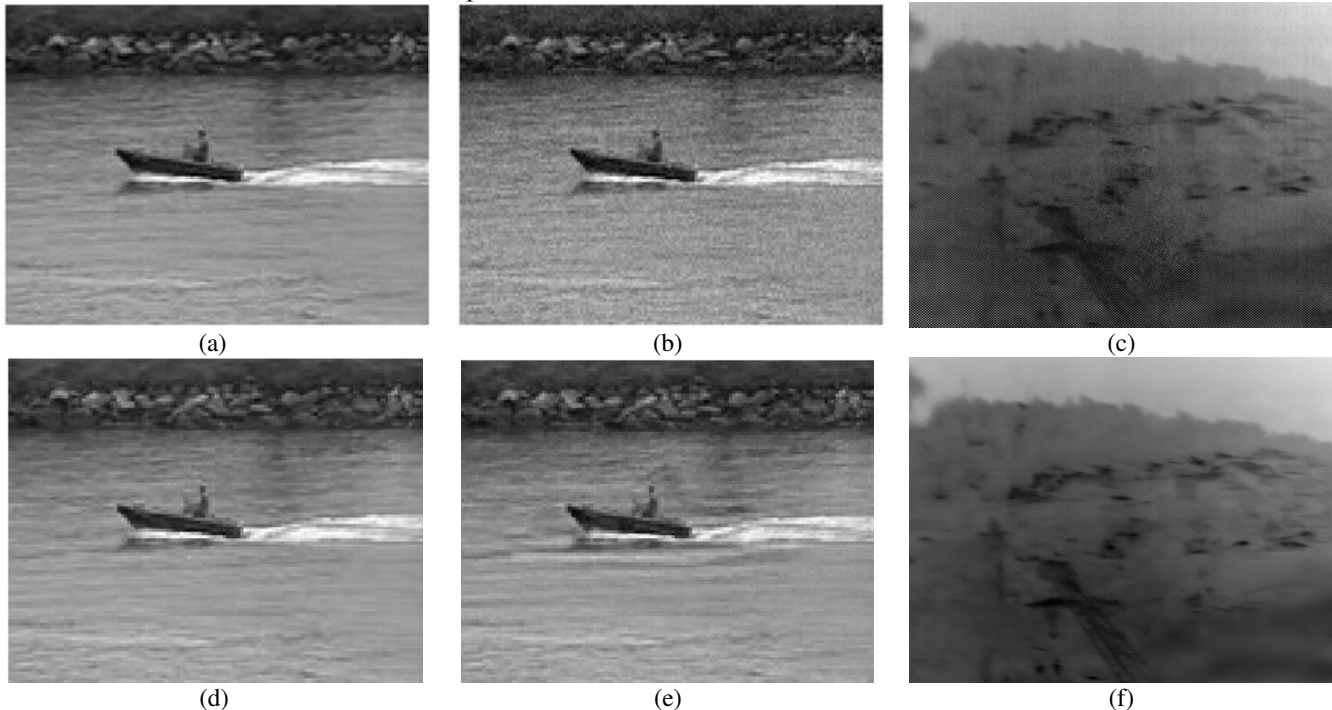


Figure 4 : (a) Original image (b) Noisy image (d) Corrected image with RNUC-GM $\eta = 0.0025$ (e) Corrected image with ANN algorithm using $\eta = 0.00035$ and block of 8 (c) Real IR image with FPN (f) Corrected image with RNUC-GM algorithm $\eta = 0.02$.

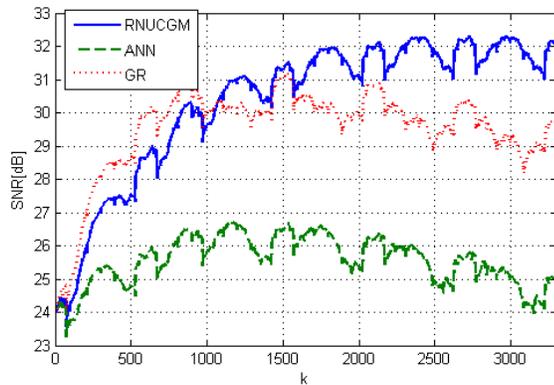


Figure 5: SNR results for synthetic video sequence corrected with: the proposed algorithm RNUC-GM (solid blue line), global algorithm with no masks GR (red dotted line) and the ANN algorithm (green dashed line).

5. ACKNOWLEDGMENT

This work was performed in the Signal and Image Processing laboratory, Dept. of EE, Technion IIT. The authors wish to thank Prof. David Malah, Nimrod Peleg and the lab staff for their help which allowed us to carry out this project.

6. REFERENCES

- [1] D. Scribner, M. Kruer, and J. Killiany, "Infrared focal plane array technology," *Proc. IEEE*, vol. 79, no. 1, pp. 66–85, 1991.
- [2] D. L. Perry and E. L. Dereniak, "Linear theory of nonuniformity correction in infrared staring sensors," *Optical Engineering*, vol. 32, no. 8, pp. 1854–1859, 1993.
- [3] A. Friedenbergl and I. Goldblatt, "Nonuniformity two-point linear correction errors in infrared focal plane arrays," *Optical Engineering*, vol. 37, no. 4, pp. 1251–1253, 1998.
- [4] J. G. Harris and Y.-M. Chiang, "Nonuniformity correction using the constant-statistics constraint: analog and digital implementations," in *Infrared Technology and Applications XXIII*, B. F. Andresen and M. Strojnik, Eds., vol. 3061 of *Proceedings of SPIE*, pp. 895–905, Orlando, Fla, USA, April 1997.
- [5] P.M. Narendra and N. A. Foss, "Shutterless fixed pattern noise correction for infrared imaging arrays," in *Technical Issues in Focal Plane Development*, vol. 282 of *Proceedings of SPIE*, pp.44–51, Washington, DC, USA, April 1981.
- [6] D. A. Scribner, K. A. Sarkady, J. T. Caulfield, et al., "Nonuniformity correction for staring IR focal plane arrays using scene-based techniques," in *Infrared Detectors and Focal Plane Arrays*, E. L. Dereniak and R. E. Sampson, Eds., vol. 1308 of *Proceedings of SPIE*, pp. 224–233, Orlando, Fla, USA, April 1990.
- [7] D. A. Scribner, K. A. Sarkady, M. R. Kruer, J. T. Caulfield, J.D. Hunt, and C. Herman, "Adaptive nonuniformity correction for IR focal-plane arrays using neural networks," in *Infrared Sensors: Detectors, Electronics, and Signal Processing*, T.S. Jayadev, Ed., vol. 1541 of *Proceedings of SPIE*, pp. 100–109, San Diego, Calif, USA, July 1991.
- [8] M.M.Hayat, S.N. Torres, E. E. Armstrong, S. C. Cain, and B.Yasuda, "Statistical algorithm for nonuniformity correction in focal-plane arrays," *Applied Optics*, vol. 38, no. 5, pp. 772–780, 1999.
- [9] S. N. Torres and M. M. Hayat, "Kalman filtering for adaptive nonuniformity correction in infrared focal-plane arrays," *Journal of the Optical Society of America A*, vol. 20, no. 3, pp. 470–480, 2003.
- [10] D. A. Scribner, K. A. Sarkady, M. R. Kruer, et al., "Adaptive retina-like preprocessing for imaging detector arrays," in *Proceedings of IEEE International Conference on Neural Networks*, vol. 3, pp. 1955–1960, San Francisco, Calif, USA, March-April 1993.
- [11] E. Vera, S. Torres, "Fast Adaptive Nonuniformity Correction For Infrared Focal-Plane Array Detectors", *EURASIP Journal on Applied Signal Processing* 2005:13, 1994–2004 2005.
- [12] B. M. Ratliff, M. M. Hayat, and R. C. Hardie, "Algebraic scene-based nonuniformity correction in focal plane arrays," in *Proceedings of the SPIE: Infrared Imaging Systems: Design, Analysis, Modeling, and Testing XII*, G. C. Holst, ed., 4372, pp. 114–124, The International Society for Optical Engineering, (Orlando, FL), Sept. 2001.
- [13] B.M.Ratliff, M.M. Hayat, and R.C. Hardie, "An algebraic algorithm for nonuniformity correction in focal-plane arrays", *Journal of the Optical Society of America A*, vol. 19, no. 9, pp. 1737–1747, 2002.
- [14] B. M. Ratliff, M. M. Hayat, and J. S. Tyo, "Generalized algebraic scene-based nonuniformity correction algorithm," *Journal of the Optical Society of America A*, vol. 22, no. 2, pp. 239–249, 2005.
- [15] S. Lim, A. El Gamal, "Gain fixed Pattern Noise Correction via Optical Flow", *IEEE Transactions on Circuits and Systems I: Regular Papers*, vol. 51, no. 4, APRIL 2004.
- [16] Irani, M. and Peleg, S., "Super Resolution From Image Sequences", *ICPR-C* 1990, vol. 90 pp. 115-120.
- [17] Michal Irani and Shmuel Peleg, "Improving resolution by image registration", *CVGIP: Graphical Models And Image Processing* Vol.53, No.3, May, pp. 231-239, 1991.
- [18] Berthold K.P. Horn and Brian G. Schunck, "Determining Optical Flow", Artificial Intelligence Laboratory, Massachusetts Institute of Technology, Cambridge, MA 02139, U.S.A.
- [19] D. Donoho. "De-noising by soft thresholding" *IEEE Transactions on Information Theory*, 41(3):613–627, 1995.
- [20] www.sipl.technion.ac.il/Info/Downloads_DataBases_e.shtml, Oct. 2007
- [21] Douglas L. Jones, "The LMS Adaptive Filter Algorithm", Connexions website <http://cnx.org/content/m11829/latest/>, Feb 2007.